

# CONSIDERATIONS FOR REHABILITATING A STEEL SELF-ANCHORED SUSPENSION BRIDGE – A CASE STUDY

## Introduction

The Andy Warhol Bridge (formerly known as the Seventh Street Bridge) is a self-anchored suspension bridge carrying Seventh Street over the Allegheny River in downtown Pittsburgh, Pennsylvania. The bridge is owned and maintained by the Allegheny County Department of Public Works, and the adjoining streets are owned and maintained by the City of Pittsburgh.

The Andy Warhol Bridge is one of the Three Sisters, the only trio of identical, side-by-side bridges anywhere in the world. The Three Sisters are composed of the Roberto Clemente, Andy Warhol, and Rachel Carson Bridges (formerly known as the Sixth, Seventh, and Ninth Street Bridges, respectively).

The bridge is comprised of three simple-span, multi-girder approach spans and a three-span continuous self-anchored suspension bridge main structure. The bridge crosses the Tenth Street Bypass, the Allegheny River and several riverfront trails. The span lengths are 72.80 ft, 221.36 ft, 442.08 ft, 221.36 ft, 41.95 ft and 61.45 ft, moving south to north, giving a total bridge length of 1,061 ft from face to face of the abutment backwalls. An extensive rehabilitation began in the fall of 2016 and was completed in the summer of 2018. Before this, the last major rehabilitation was completed in the mid-1990s.

The construction phase of the Andy Warhol rehabilitation presented several unique problems requiring equally unique solutions. The project offered an exceptional opportunity to learn about the bridge's history, its design, and considerations to keep in mind when designing rehabilitations for future complex bridges. Lessons learned from the first rehabilitation can be applied to the other two bridges in rapid succession.

## History

The existing Andy Warhol bridge is the second bridge at this site, replacing an earlier “traditional” externally-anchored suspension bridge designed by Gustav Lindenthal. The bridge's replacement was mandated by the 1889 River and Harbor Act, which required a minimum 47-foot vertical clearance above normal pool elevation of the Allegheny River. This earlier bridge's design also revealed challenging subsurface conditions when the northern cable anchorages began to slip toward the river and were repaired with additional masonry (1).



**Figure 1: The 1884 Lindenthal Bridge (2)**

Four bridge designs were proposed for the site, encompassing static and movable trusses as well as another externally-anchored suspension bridge. The proposals were vetoed by the Pennsylvania Public Service Commission, citing aesthetic concerns. The suspension form was favored by the public and the commission alike, despite the knowledge of the difficulty of anchoring the suspension cables near the river banks (3).



**Figure 2: Elevation of the Andy Warhol Bridge (Looking Southeast Toward Downtown Pittsburgh)**

The only bridge type capable of meeting the demands of all the involved parties was a self-anchored suspension bridge. At this time, only one existed in the world, a small self-anchored span over the Rhine River in Cologne, Germany that opened to traffic in 1915. The HABS-HAER documentation for the Three Sisters Bridges notes that the news of the Cologne bridge's completion would have reached Pittsburgh at about the same time that the new bridge proposals were rejected. At that point, the self-anchored suspension bridge became the favored bridge, and the resulting design would be the first self-anchored suspension bridge in the United States (4).

The credit for the actual design of the bridge is not easy to pinpoint; the available design calculations are unsigned and unsealed. Credit for the design is typically attributed to the Allegheny County Engineer, Vernon Royce Covell. However, consulting engineering Thomas Wilkerson (who was responsible for designing many of the major river crossings in the Pittsburgh area) directly took credit for the design on at least one occasion (5).

The proposed bridge typical section included two-12-foot-wide sidewalks supported by overhang brackets (outboard of the suspension chain), a single lane in each direction for vehicular traffic, and two trolley tracks along the center of the roadway. These trolley tracks remained in service until 1967 when trolley service was discontinued. The tracks were removed in a subsequent rehabilitation and the

bridge was reopened to four-lane bi-directional traffic.

The American Bridge Company of Ambridge, PA (approximately 16 miles downriver on the Ohio River from Pittsburgh) and the Foundation Company of New York were chosen to construct the Seventh Street Bridge (and the companion spans at Sixth Street and Ninth Street). Because of restrictions on how much the Allegheny River navigation channel could be reduced, American Bridge decided to erect the bridge as a cantilever. At the time, this approach was not uncommon for erection of common cantilever trusses but was entirely unheard of for the erection of a suspension bridge.

Because rock lies approximately fifty to sixty feet below ground at the bridge's location, a temporary anchorage to solid material was considered but ultimately discarded. The use of falsework was an obvious solution, but the decree of the War Department included a provision that the Allegheny River be kept navigable at all times. Therefore, the American Bridge Company suggested erecting the bridge as a cantilever, using temporary bents outside of the main channel and a system of temporary members to stiffen the suspension structure into a truss (6)

Temporary timber pile bents were constructed in the river, and temporary struts were placed within the panels of the suspension system. Thus, the bridge was erected essentially as a cantilevered truss. A series of hydraulic jacks acting on the temporary struts allowed the structure to be manipulated

enough to install the entire suspension chains, stiffening girders and floor system. When the final segments of the suspension chains and stiffening girders were set in place and the hydraulic jacks released, the temporary supports loosened and fell away, leaving the bridge in its anticipated dead-load geometry (7).

## Mechanics of the Self-Anchored Suspension Bridge

The self-anchored suspension bridge is a unique structural system, both in form and its relatively rare use. As in the traditional suspension form, the deck and stiffening girders (or trusses) are hung from the suspension cable or chain by hangers, and the cables transmit this load to the supports by axial tension. In a self-anchored form, the cable is anchored to the end of the stiffening girder instead of securing the cable to massive masonry anchorages. The cable tension is therefore resisted directly by axial compression in the stiffening girder. In addition to axial compression, the stiffening girder is also subjected to flexure arising from local bending between hangers as well as the eccentric action of the thrust at its ends (see Figure 3). The self-anchored suspension bridge is more like an inverted tied arch than a suspension bridge in terms of the forces to which its components are subjected.

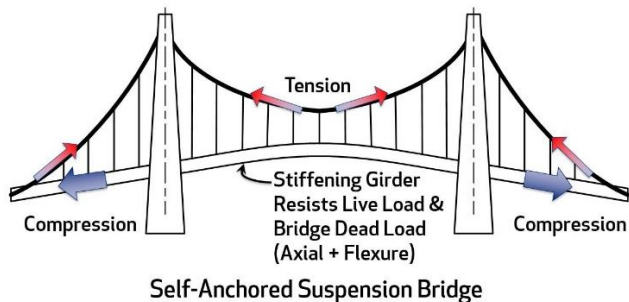


**Figure 3: General Flow of Forces in a Self-Anchored Suspension Bridge**

Because the suspension cables/chains are anchored to the ends of the girder, the need for massive end anchorages is eliminated, and instead the stiffening girders must be sized for the required axial and flexural resistances. Tie-down assemblies must be provided at the ends of each stiffening girder to resist the uplift due to dead and live loads as well as some amount of compression due to the reactions of the end floorbeams. This allows the use of a

suspension bridge in areas of difficult subsurface conditions or where the available right-of-way precludes the use of large end anchorages (both reasons for using the self-anchored form for the Three Sisters).

Of note is the fact that the end anchorages of the suspension spans of the Three Sisters are not actually at the riverbanks; due to riverfront roadways and railroad tracks (at the time of original construction) there are short approach spans at each end of the main suspension unit. The designers therefore chose to anchor the tie-down assemblies to a steel grillage at the bottom of the piers and to use the mass of the pier itself to resist the uplift at the ends of the suspension spans.

Several key assumptions must be made about the geometry and behavior of a self-anchored suspension bridge. In a traditional elastic analysis, the following six assumptions may be made (8):

1. The curve of the main cable/chain is parabolic.
2. The stiffening girder camber (if any) is also parabolic.
3. Dead load is uniformly distributed in each span.
4. The hangers are vertical and remain vertical while deflecting.
5. The hangers are inextensible.
6. The moment of inertia of the stiffening girder is constant in any given span.

These six assumptions are typically untrue. Assumptions (1), (2), (3), and (6) simplify the analysis by reducing the number of unknowns to be considered in the analysis. Note that these assumptions are only necessary for analyzing the bridge by hand; the power of modern computing and finite element analysis allows the bridge to be precisely modeled. Upon examining the behavior of the bridge in its final position when subjected to loads, the effects of the bridge's deflections and rotations is usually small enough to ignore without a large loss of accuracy of the solution, which is incorporated into the analysis by assumptions (4) and (5).

The stiffening girder and bridge deck may be laid out as flat (or on a straight grade) or with a parabolic vertical curve/camber. A parabolically-cambered stiffening girder carries applied load in both axial

compression and flexure. If the bridge is laid out for the dead load camber during fabrication, there should be no dead load moment in the stiffening girder other than the girder's self-weight between hangers and moment that results from the girder being continuous through the towers. This is a direct result of the arching action of the cambered girder, which results in a portion of the dead load being carried by axial compression.

Live load deflections in a self-anchored suspension bridge are offset by an increase in the suspension chain tension and a decrease in the stiffening girder compression. The reason for this is, by the assumption that the hangers are inextensible, the deflection of the stiffening girder must be equal to the deflection of the suspension chain. This is observed by drawing a free-body diagram of one-half of the main span and summing moments about the tower. This is presented below in Figure 4. The solid lines in the figure represent the original bridge position, and the dashed lines the deflected shape.

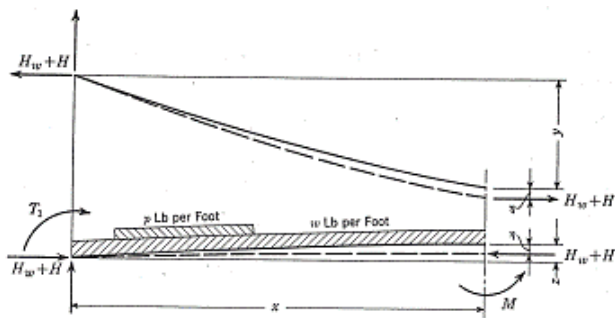


**Figure 4: Self-Anchored Suspension Bridge Live Load Deflections (4)**

Where the variables in Figure 4 are defined as follows:

- $H_w$  Horizontal component of dead load axial force (kips)
- $H$  Horizontal component of live load axial force (kips)
- $T_1$  Moment due to girder continuity through the tower (kip-feet)
- $p$  Distributed live load (kips/foot)
- $w$  Distributed dead load (kips/foot)
- $x$  Position along main span (feet)
- $y$  Vertical position of cable at  $x$  (feet)
- $z$  Vertical position of girder at  $x$  (feet)
- $\eta$  Vertical deflection at  $x$  (feet)

The stresses that would be caused by the deflection of the stiffening girder are reduced by the simultaneous changes in the stiffening girder moment caused by the total compression,  $H_w + H$ , multiplied by the deflected  $z$ . By assuming the suspenders are inextensible, the quantities  $(y + z)$  and  $(f + a)$  remain constant, so the value of  $H_w$  does not change. Subsequently, under the aforementioned assumptions only, a self-anchored suspension bridge may be analyzed by using the elastic theory, since the changes in forces are not greatly affected by changes in the structure geometry. This analysis may then be considered linear and superposition is valid, allowing influence lines to be constructed for various loading conditions.

An alternative to the elastic theory of analysis is the deflection theory. The deflection theory for suspension bridges accounts for the changes in the cable curvature under load, and these changes in geometry lend increased stiffness to the suspension system (sometimes referred to as “stress-stiffening”). The deflection theory considers both the elastic stiffness of the individual bridge elements and the geometric stiffness resulting from the bridge's deflected shape. The resulting equations of equilibrium are nonlinear, and their solutions require the use of iterative solutions to update the system of forces within the suspension system. As demonstrated before, because the self-anchored suspension bridge is not made stiffer by live load deflections, the effects of the deflections may be ignored, and the bridge analyzed by the elastic theory (9).

The original design utilized the elastic theory, considering the bridge on a flat grade and introducing a “correction” to account for the camber of the stiffening girder, i.e., the arching action that the girder provides. The final cambered geometry of the bridge was determined by using the full dead load and one-half of the design live load. Thus, under the dead-load only condition, the bridge is over-cambered, which induces additional flexure in the stiffening girders. Furthermore, the attachment between the suspension chain and stiffening girder is not located at the center of gravity of the girder, thus inducing additional flexure at the girder ends due to the eccentricity of the connection.

The significance of the arching action is observed by examining the difference in girder/cable force when

excluding the girder camber,  $a$ , in the calculations of the horizontal component of the girder/cable force. In his discussion of the paper *Self-Anchored Suspension Bridges* by Oschendorf and Billington, Wollman (10) formulates the difference in cable forces as a simple ratio (reproduced here as Equation 1):

$$p - 8h_1 \frac{f}{l^2} = p - 8h_2 \frac{f}{l^2} - 8h_2 \frac{v_0}{l^2} \quad \text{Eqn. 1}$$

Equation 1 Eqn. equates the horizontal cable forces in a bridge with a flat stiffening girder (left side of the equation) and a bridge with a cambered stiffening girder (right side of the equation). Dropping the equivalent terms and rearranging yields:

$$\frac{h_1}{h_2} = 1 + \frac{v_0}{f} \quad \text{Eqn. 2}$$

Where  $(h_1/h_2)$  is the ratio of cable/girder axial forces of a flat bridge to a cambered bridge,  $v_0$  is the main span girder camber, and  $f$  is the cable sag (6). Using the values from the original Seventh Street design plans (reproduced later) gives:

$$\frac{h_1}{h_2} = 1 + \frac{7.33 \text{ ft}}{55.24 \text{ ft}} = 1.13$$

Consequently, including a girder camber of 7.33 ft in the Andy Warhol Bridge yields a 13% decrease in the axial force in the stiffening girder.

## Analysis

During review of the available original calculations, it was observed that there were two mistakes made in the calculation of the anchor span end reactions. First, the dead load reaction was originally calculated to be 33.2 kips downward, i.e., “compressive.” This calculation sheet is marked “Copied & Revised” and was superseded by a sheet giving the dead load reaction as 126.3 kips downward. The revised dead load reactions never made it onto the original design drawings, which show the 33.2-kip reaction. The second mistake was the process of calculating the reactions themselves. The dead load reactions were found by summing the dead load moments about the tower and dividing by the anchor span length. However, the values used in the calculation consider only the loads on the stiffening girder and not the effects of the suspension

chain or the axial compression within the stiffening girder itself.

To verify, construct a free-body diagram of Panel Point 0, including the end anchorage, the suspension chain, and the stiffening girder and cut a plane through the stiffening girder and suspension chain (see **Error! Reference source not found.**). For this joint to be in equilibrium, the horizontal components of  $F_{chain}$  and  $F_{girder}$  must be equal and opposite, and the sum of the vertical components of  $F_{chain}$  and  $F_{girder}$  and  $R_{PP0}$  must equal zero.

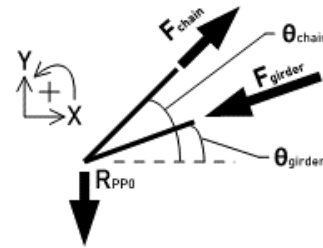


**Figure 5: Free-Body Diagram of Panel Point 0**

Considering only the dead loads, another free-body diagram may be constructed of one-half of the main span and moments summed about the centerline of the main span. Considering a uniformly-distributed dead load,  $w$ , acting in the main span and solving for the horizontal component of the axial loads in the suspension chain and girder yields Equation 3:

$$H_w = \frac{wL^2}{8(f + a)} \quad \text{Eqn. 3}$$

Where  $w$  is the dead load in kips per foot,  $L$  is the main span length in feet,  $f$  is the main span cable sag in feet, and  $a$  is the maximum camber of the main span stiffening girder in feet. Using values from the original design calculations:  $w = 8.392$  kip/ft,  $L = 442.08$  ft,  $f = 55.25$  ft, and  $a = 7.33$  ft yields:

$$H_w = \frac{8.392 \times 442.08^2}{8(55.25 + 7.33)} = \pm 3,276 \text{ kips}$$

Using the design bridge geometry,  $\theta_{chain} = 6.94^\circ$  and  $\theta_{girder} = 2.39^\circ$ . This gives, by geometry, the vertical components of  $F_{chain} = +399$  kips and  $F_{girder} = -137$  kips, giving  $R_{PP0} = +262$  kips, a net dead load uplift (the positive sign of  $R_{PP0}$  indicates that its direction is consistent with that assumed in Figure 5). Examining prior plan sets used in various

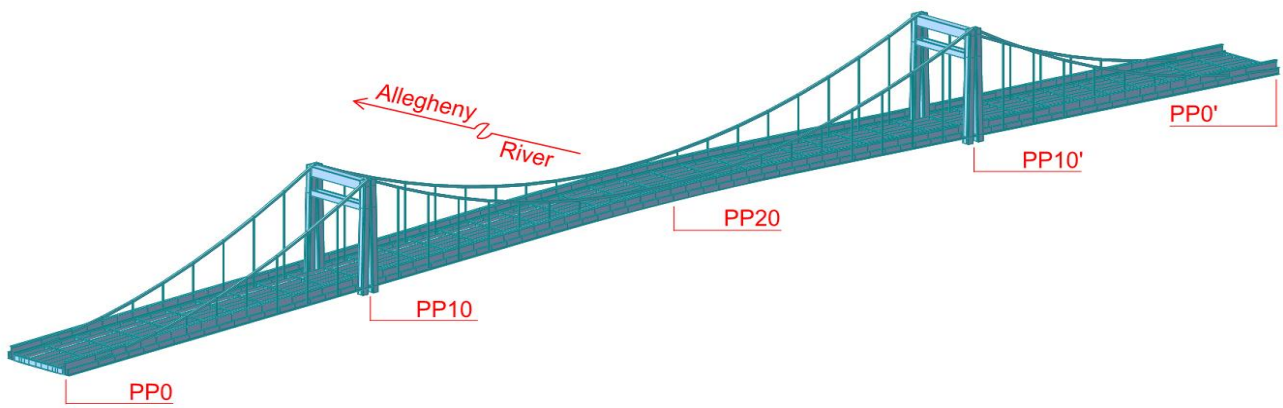


**Figure 6: Isometric View of Midas/Civil Finite Element Model**

rehabilitations, it was noted that some of the plan sets showed the incorrect reaction of 33.2 kips.

### Finite Element Modeling

An annotated view of the Midas/Civil finite element model is given in Figure 6 on the following page. The primary focus of the finite element analysis of the bridge was to determine the initial dead load forces in the bridge. The secondary focus of the analysis was to examine the effects of laterally-unbalanced load and the magnitude of the effects of large crowds of pedestrians.

All element cross-sections were modeled using their as-built properties (without considering any deterioration). The stiffening girder sections were drawn in Microstation and imported into the Midas Section Designer. There, the section properties of the complex sections were calculated and exported into Midas/Civil as general sections. The calculated properties were then compared to the original design sections properties for validation before continuing.

The bridge was modeled in its dead-load-only position, i.e., the bridge was modeled in its desired geometry after all dead loads had been applied and all dead load deflections have taken place. In this state, the bridge undergoes only small deflections and thus there is no appreciable difference between the deformed and undeformed geometries. This presents a problem when analyzing cable-supported structures: the final geometry of the bridge is typically known ahead of time (profile, vertical curves, cable sag, etc.) but the undeformed or initial position of the bridge is unknown. If the structure were modeled in this position and the self-weight is then applied (“turning gravity on”) the bridge will

deflect beyond its final position and the analysis results would be incorrect.

Because the bridge geometry changes during construction as the bridge moves toward its final position, linearized analysis is not appropriate for analyzing the structure. A geometrically-nonlinear analysis is required to properly capture the changes in stiffness of the bridge as a result of its deflections. There are two numerical methods to solve this problem: (1) the initial shape of the bridge is found using shape-finding algorithms, the bridge is modeled in this position, self-weight loads are applied, and the bridge can deflect into its final dead-load-only position, or (2) model the bridge in its desired final geometry and determine the system of internal forces that results in force equilibrium in that geometry. Both (1) and (2) are methods of incremental, geometrically-nonlinear analysis which will result in the same final answer. The Midas/Civil Suspension Bridge Analysis Control Module (SBAC) uses Method (2), which was the chosen method of analysis (also, the desired dead-load geometry was well-annotated in the existing plans and gave an excellent reference point).

By inputting the final bridge geometry, bridge self-weight, and applied dead loads, the Midas SBAC internally calculates the element forces that result in equilibrium for the prescribed geometry and loading. The system of forces determined by Midas/Civil are the forces that result in no deflection under self-weight of the model. These forces are included in any further analyses as geometric stiffness that is added to the individual element stiffness. Because accurate drawings were available, it was decided to model the bridge in its original, as-built state. After determining the initial element forces, additional loads would be defined to reflect the changes in dead

load due to the numerous rehabilitations undertaken since 1926.

The Midas/Civil model of the bridge included the suspension chains, hangers, stiffening girders, towers, and floor system. The decision was made to not model the existing deck because it was noncomposite. The resistances of the newly-composite floor system members were calculated externally using other software. The deck was omitted to eliminate participation of the deck in the strength of the suspension system the floor system was included only to obtain the self-weights to apply to the suspension system and to provide convenient locations to define live loads. The dead load of the existing and proposed decks was applied as distributed loads on each of the stringer lines.

In the floor system, the rolled-shape stringers are simply supported at the faces of the floorbeams, and the floorbeams are simply supported by the stiffening girder. All the structure dead loads and live loads (aside from self-weight) are applied to the stringers. This would have been the original designers' intent, as the primary purpose of the stiffening girder would then be to provide stiffness to the deck in between each panel point hanger and the majority of the loads would manifest as axial forces in the suspension system. This is analogous to the design of a truss, where live loads and the dead loads of the deck and floor system are applied as point loads to the trusses at the floorbeam locations.

The self-weight dead loads entered in the Midas/Civil SBAC include the dead loads calculated by the original designers and one-half of the original design live load. An excerpt of the original dead load calculation summary is given in Figure 7. In Figure 7, the individual bridge elements are tabulated in units of pounds per linear foot, per girder line. To replicate the forces the engineers used in the original analysis, one-half of the design live load is added to the figures shown in Figure 7. This results in a structure "self-weight" of 10.040 kips/ft in the main spans and 11.183 kips/ft in the anchor spans. These loads were reduced to account for self-weight of the elements in the finite element model (which can be accounted for directly) and the resultant line loads were applied to the stringers and girders as "element" or line loads.

	ANCHOR ARM	MAIN SPAN
<i>Sidewalk Slab</i>	876 LBS.	876 LBS.
<i>Roadway Pavt.</i>	665 "	665 "
" <i>Base</i>	1188 "	1188 "
<i>Tracks &amp; Fast's</i>	90 "	90 "
<i>Sidewalks I<sup>s</sup></i>	26 "	26 "
" <i>Brackets</i>	54 "	54 "
<i>Fascia Girders</i>	58 "	58 "
<i>Floor Beam</i>	428 "	428 "
<i>Floor System</i>	524 "	524 "
<i>Teleph. Conduit</i>	360 "	360 "
<i>Gas Line</i>	90 "	90 "
<i>Trolley Poles</i>	13 "	13 "
<i>Cables</i>	1074 "	1020 "
<i>Hangers</i>	51 "	51 "
<i>Girders</i>	3956 "	2886 "
<i>Cast St. Expt.</i>	18 "	" "
<i>Handrail</i>	64 "	64 "
<b>TOTAL</b>	<b>9535 "</b>	<b>8392 "</b>

**Figure 7: Excerpt from the original dead load calculations (Units are lbs/ft per girder line) (11)**

Once the initial element forces were determined, additional static load cases were developed to reflect changes in the structure dead load over its service life. The load cases applied reflect the replacement of the original deck, various structural steel repairs, removal of the trolley line elements, and the proposed rehabilitation dead loads, including the new, heavier reinforced concrete deck, utilities, and an allowance for a future wearing surface.

The resultant forces were used in all design and load rating calculations. Separate Midas/Civil models were developed for each of the following live load considerations:

- Moving live loads, including PennDOT design and load rating vehicles and pedestrian loads.
- Static live loads, including wind on live load, wind on structure, and temperature change.
- Construction sequencing, including removal of the existing deck and placement of the new deck.
- Pedestrians-only case, where the bridge is closed to vehicular traffic and used exclusively by pedestrians.

The final case is a special load case developed for analysis to examine the effects of large crowds of pedestrians on the structure. Because of their proximity to downtown Pittsburgh, Heinz Field (Pittsburgh Steelers), and PNC Park (Pittsburgh

Pirates), the Three Sisters bridges are occasionally closed to vehicles and the bridges are used to allow pedestrian access, stage fireworks, or to provide space for concerts and concessions. Pedestrian loads are input as moving lane loads and are moved longitudinally to produce maximum force effects. Transversely, the pedestrian load was applied on each sidewalk, each half of the roadway, and various combinations of the two. It is of note that because of the space available to pedestrians, these lane loads exceed the lane load of the HL-93 design loading.

It was observed that factored load cases including wind and temperature changes do not control the load ratings of the suspension system or stiffening girder, compared to load cases including vehicular and pedestrian loads. It was also noted that the Midas model verified that there is a permanent dead-load uplift at the ends of the anchor spans. The Midas value of the uplift was -275.6 kips, compared to the -262 kips calculated earlier, a difference of less than 5%.

### Elastic Theory Verification

The finite element analysis was verified by use of the elastic theory to determine the initial element forces (dead loads). After a significant amount of research, the best resource discovered was the paper *Simplified Theory of the Self-Anchored Suspension Bridge*, which was a thesis paper submitted by Carl H. Gronquist to Rutgers University in 1940, in fulfillment of his civil engineering degree. Gronquist provides an extensive examination of the theory behind a self-anchored suspension bridge and a summation of the suspension bridge design resources available at that time. The nonlinear finite element analysis results were not expected to agree exactly with those from the elastic theory; however, as previously discussed, for a self-anchored suspension bridge the results would be sufficiently accurate to determine if the results from the finite element analysis were reliable.

By the assumption that there is no dead load moment in the stiffening girder, the horizontal component of the tension or compression in the suspension system may be obtained using Equation 3. This assumption is contingent on assuming that the bridge is laid out during fabrication such that all the dead-load deflections are zero. As the first check of the theory against the finite element analysis results, the axial forces in the suspension chain were checked. By

geometry, the maximum axial forces would occur in member U9-U10 (the last suspension chain element in the anchor span). Using the values previously given and substituting 10.040 kips/ft for  $w$  (the original dead load plus one-half the design live load) gives  $H_w = 3,919$  kips. A summary of the calculated forces in element U9-U10 is given in Table 1.

**Table 1: Comparison of Axial Forces in Element U9-U10 (Units of kips)**

Method of Analysis	Elastic Theory	FEA Model	Original Plans
Dead Load Axial Force	4,606	4,210	4,328
% Difference	---	-8.5%	-6.4%

The equation giving the moment in the stiffening girder at any point in the main span is given below as Equation 4 (reproduced from Gronquist). This equation relates the quantities shown in Figure 4 earlier.

$$M = T + M_D + M_0 - (H_w + H) - (H_w + H)(z - \eta) \quad \text{Eqn. 4}$$

Where  $M$  is the total moment acting on the stiffening girder at any section  $x$ ,  $T$  is the bending moment at any section  $x$  due to continuity of the stiffening girder,  $M_D$  is the dead-load bending moment considering the girder as a simple beam, and  $M_0$  is the simple-beam bending moment due to a live load,  $p$ . Recall that in Equation 4, the  $\eta$ -terms cancel due to the assumption of inextensible hangers. Ignoring the live load terms yields Equation 5:

$$M = T + M_D - H_w(y + z) \quad \text{Eqn. 5}$$

If the stiffening girders were hinged at the towers, all the global dead load moments would vanish as the girder self-weight moments would be negated by the uniformly-distributed hanger forces. The only dead load moments in the girder would then be due to its self-weight between the hangers. In the case of a stiffening girder continuous through the towers, moments due to continuity appear. The  $T$ -term is the moment in the stiffening girder at the tower due to its continuity and was derived using Clapeyron's Theorem of Three Moments for various loading conditions, including distributed loads in either the anchor or main span, concentrated loads traversing either span, and applied concentrated moments at the



ends of the anchor spans (12). Generalized and written to reflect the moment in the girder in the main span we write:

$$M(x) = \{M\} + H[e(x)(f + a) - (y(x) + z(x))] \quad \text{Eqn. 6}$$

In Equation 6, the  $e(x)$  term is the coefficient of continuity that may be determined through the Theorem of Three Moments and  $M\{x\}$  is the summation of the moment due to continuity and simple-beam bending moment from live load. The value of  $e(x)$  varies linearly in the anchor spans from zero to  $e$  and equals  $e$  in the main span. In the case of a three-span continuous, symmetric girder hinged at its ends may be obtained using Equation 11 in Gronquist, reproduced here as Equation 7:

$$e = \frac{2 + 2irv}{3 + 2ir} \quad \text{Eqn. 7}$$

Where  $i$  is the ratio of the main span girder moment of inertia to the anchor span moment of inertia,  $r$  is the ratio of the main span length to the anchor span length, and  $v$  is the ratio of the combined main span sag and camber to the anchor span combined sag and

camber. The terms  $y(x)$  and  $z(x)$  are the ordinates of the suspension chain and stiffening girder, respectively.

## Analysis Results

As was discussed previously, the end reactions at the girder tie-downs were in excellent agreement with the finite element results, as were the tower reactions. The axial forces obtained for the suspension chain were in relatively good agreement with those shown on the original plan sheets. The largest difference was observed at element U9-U10, where the difference was approximately 8.5% as was shown in Table 1.

The stiffening girder moments obtained from the finite element model, the elastic theory, and the original plan sheets are shown in Figure 8 on the following page. The moments given in the original design plans do not correlate well with those from the analyses because they are simply the product of the girder axial force and an eccentricity, where the eccentricity is the difference between the elevation of the end pin that connects the stiffening girder to the suspension chain and the girder center of gravity at each panel point.

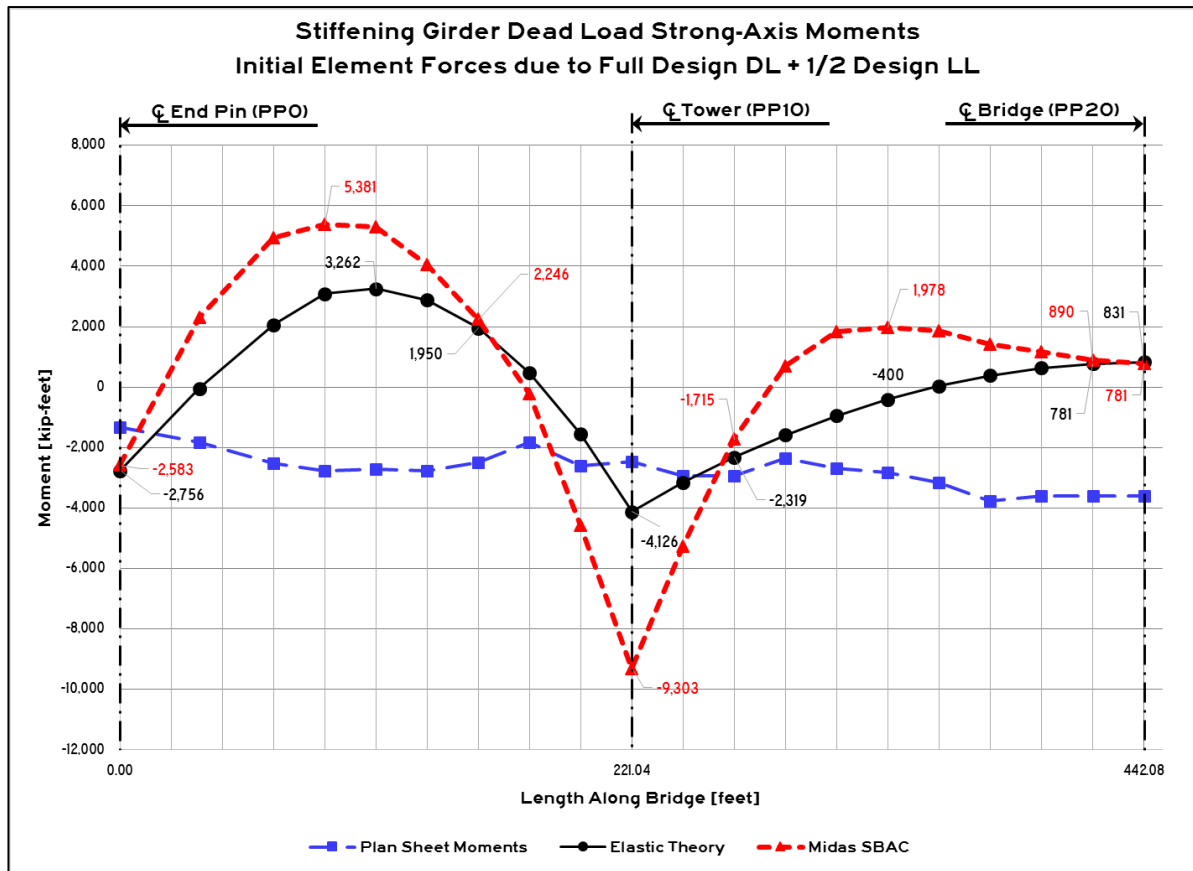


**Figure 8: Comparison of Stiffening Girder Strong-Axis Moments**

Comparing the elastic theory moments to those from the finite element analysis, the most important takeaways are that (1) the moments are of the same signs at the same locations, and (2) the moments at the free end of the girder and at midspan are approximately equal. Obtaining moment diagrams of essentially the same shape encouraged the engineers that the finite element analysis and elastic theory applied the girder end moments, the effects of the main span camber, and the equal distribution of the girder self-weight and suspension hanger reactions were relatively balanced. Recall that the bridge was laid out in its desired position under then effects of dead load plus one-half the design live load, resulting in excess camber and thus a residual moment in the stiffening girder under dead load alone.

An additional conclusion that may be drawn regarding the differences in bending moment relates to the concept of total strain energy. Since the finite element solution is a nonlinear solution, the analysis considers the conservation of strain energy within the structure as it undergoes deformation. The

difference is axial forces and bending moments may be attributed to the total strain energy developed within the system by all of the internal and external forces, namely by including the deformation due to bending in the stiffening girder which balances the work done on the structure.

A portion of the difference in the magnitude of the moment at the tower locations (PP10) may be attributed to the support condition at the tower. In the finite element model, the stiffening girder and tower legs coincide at the same node. Beam end releases were applied at this node to release the moment at this location in the tower, but the overall girder stiffness is increased due to the presence of the tower. The elastic theory assumed that the girder is pin-supported at this location, thus rotation at that point is totally unrestrained.

## Construction

During construction, there were several interesting problems that had developed over the years and needed addressed during the rehabilitation:

1. Rapid deterioration of the noncomposite deck.
2. Hidden deterioration of the tower bases.
3. A discrepancy between existing and proposed top of pier elevations at the tie-down locations.
4. Unanticipated movement of the bridge during the end tie-down replacements.

Each of these will be discussed in detail.

### **Rapid Deterioration of the Noncomposite Deck**

The Three Sisters Bridges, as with many other bridges of the era, did not employ composite construction of the deck and floor system to resist applied loads. Instead, the bridge floor consists of a lightly-reinforced noncomposite concrete fill supported by steel buckle plates. The buckle plates, in turn, are supported by the stringers and floorbeams, which transfer the applied loads to the suspension system. In this system of construction, the noncomposite deck does not act in conjunction with the supporting floor system to directly resist live load; its function is simply to provide a riding surface for traffic. The applied loads are resisted by the buckle plates, which are riveted around their perimeters to the stringers and floorbeams.

A drawback of this construction form is that the entirety of the concrete fill is not positively attached to the floor system in any way. If the bridge is flexible enough, the concrete fill tends to “float” over supporting floor system. Normally, this is not a concern in truss and girder bridges as the bridge is stiff enough globally to resist the tendency of the bridge to deflect, especially laterally. At some unknown point in the past, the lateral bracing under the Three Sisters Bridges was cut away. Since the lateral stiffness of the bridges was then reduced, the result is that the concrete fill floats over the surface of the supporting floor system, effectively grinding the bottom of the concrete into dust. This problem had been addressed numerous times by the County Department of Public Works, whose maintenance crews were a constant presence on the bridge filling and patching potholes. Anecdotes from County employees indicated that the bottom two- to four-inches of the concrete deck was essentially gravel and dust instead of a cohesive concrete matrix.

Considering the existing maintenance issues – and desiring to take advantage of the increased flexural resistance that composite construction offers – the

existing stringers and floorbeams were made composite using bolted channel and welded stud shear connectors. Separate approaches had to be used for the stringers and floorbeams as a result of their construction and chemical compositions.

Since the stringers are small rolled beams, the riveted connections of the buckle plates to the stringer top flanges left no room to physically weld shear studs to the stringer itself. Additional analysis showed that studs could not be simply welded to the buckle plates, as the shear strength of the riveted connection between the buckle plates and stringers would limit fully composite action. Instead, channel-type shear connectors were designed using the provisions of the *AASHTO LRFD* code. Instead of welding, rows of rivets at the desired pitch along the stringers were removed and the channels were attached using same-diameter high-strength bolts. The flanges of the floorbeams were wide enough to weld two rows of traditional shear studs.

### **Hidden Deterioration of the Tower Bases**

The suspension towers of the Three Sisters bridges are essentially two I-shaped posts set against each other at an angle. The space between the two posts is hollow so that the stiffening girder can pass through the towers at the roadway level. The tower interiors are protected from the roadway by a solid cover plate and a curb plate at the roadway level. Over time, the curb plates deteriorated away due to the constant presence of moist debris and salt-laden water. The resulting holes allowed saltwater to leak through the towers and, over several decades, caused severe section loss and deterioration of the interior tower diaphragms and tie rods.

During construction, eight 2-inch diameter tie rods and tapered wedges were used per tower leg to maintain the geometry of the built-up tower legs and were locked in place by hex nuts when construction was completed. In order to make sure that the stiffening girder was completely seated within the tower bases at Panel Points 10 and 10', a tapered steel casting was used with wedge plates that allowed the casting to slide downward until all of the material in the tower was completely seated on the pin at the base of the tower. These rods were used to resist the forces that tended to splay the tower legs apart at their bases.

These rods were severely deteriorated where they passed through the tower plates. The worst-case losses resulted in the rods being reduced from two inches in diameter to ¾-inch diameter, resulting in an 86% loss of cross-sectional area (see Figure 9 on the following page). In the figure, the red arrows indicate the full section of the tie rods and the blue arrows indicate the worst-case section loss of the tie rods.

Four of these rods could not be replaced due to the geometry of the finished bridge, so the four accessible rods were replaced with 2-inch diameter ASTM A709 Grade 36 rods which, when combined with the remaining rods, exceeds the strength of the original eight rods. Interior diaphragms, used to keep the tower plates at the proper distance apart, had also deteriorated into dust and were replaced in kind.

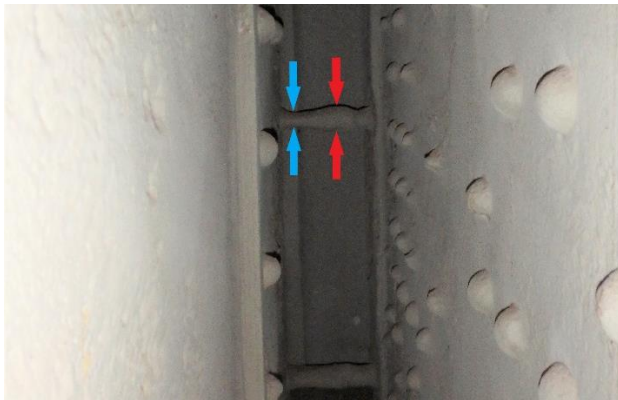


**Figure 9: Worst-Case Section Loss of 2-inch Diameter Tower Tie Rods**

### **Discrepancy Between Existing and Proposed Top of Pier Elevations**

In the prior sets of design plans, the top of pier elevation was noted as 730.39 for Piers 1 and 4 of the Andy Warhol Bridge. These elevations were carried through this rehabilitation and were used to set the length of the splices between the existing tie-down material and the new tie-downs. However, when the new tie-down assemblies were installed, the masonry plates of the assemblies were set below the top of the existing pier. In addition, the Pier 1 steel tooth dam and the Pier 4 neoprene strip seal dam were obviously misaligned vertically, with the approach spans approximately 1 inch higher than the adjacent suspension span. Measurements taken in

the field confirmed that all the new tie-down material was fabricated per the design plans.

An exhaustive search of the existing plan sets for all three bridges turned up a minute detail in the shop drawings of the approach span bearings that were used in the 1990s rehabilitation. When repairs were undertaken at the tie-down locations and the adjacent approach span bearing pedestals, a thin concrete overlay was placed on the piers to provide a level bearing surface for new approach span pedestals and the tie-down bearing assemblies. The difference – approximately 1 inch – was the exact difference in elevation between the actual top of pier surface and the proposed masonry plates.

To rectify the situation, the existing splice plates were removed and re-fabricated with a set of shop-drilled holes to fasten the splice plate to the bottom portion of the tie-down assembly. The remainder of the holes were then field-drilled using the existing material as a template (see Figure 10). In the figure, the splice plate of interest is outlined in red. The top eight holes of this plate were drilled in the field using the new tie-down material as the template. In this way the bridge could be jacked to the proper elevation at each end and the tie-downs drilled and bolted to fix the bridge end at the correct elevation.

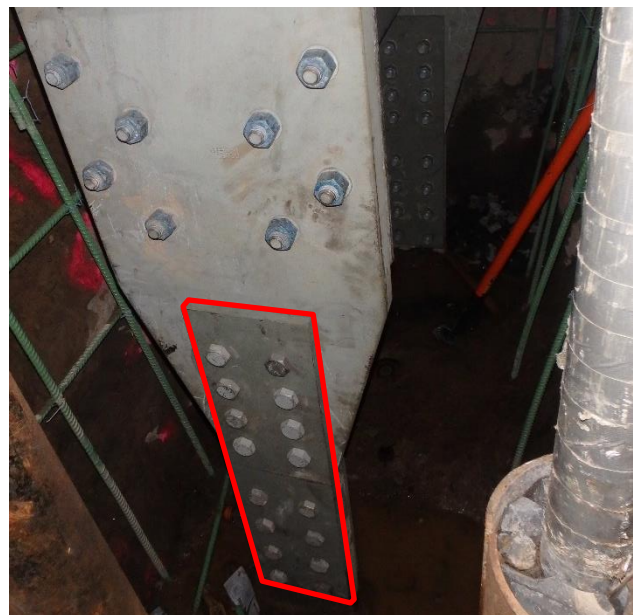


**Figure 10: Splice Plates of Tie-Down Assembly**

### **Unanticipated Movement of the Bridge During Tie-Down Replacements**

Finally, this issue was the most important one uncovered during construction (and carried the most negative consequences unless addressed properly).

During design, it was recognized that the ends of the bridge would have to be temporarily supported in some way so that the permanent tie-down assemblies could be removed and replaced. A sample detail was developed and included with the design drawings, with the actual design of the temporary support system left up to the contractor. The temporary system used for construction included timber and steel cribbing underneath the stiffening girders and an enormous “hold-down” weldment atop the stiffening girder, anchored to the pier below using post-tensioning bars drilled and grouted into the pier below. Other work included the excavation of a pit in the concrete core of the pier to fully expose the anchorage assembly so that it could be dismantled and removed.

When the existing tie-down material was severed, the ends of the bridge dropped approximately  $\frac{3}{8}$ -inch and came to rest atop the cribbing, instead of raising upward against the hold-down as anticipated. Visits to the site confirmed that all the post-tensioning rods, each capable of resisting the estimated 200 kips in tension each with capacity to spare, were completely slack.

An exhaustive effort over several days failed to identify the lack of uplift. At this point in time, the bridge was in an intermediate state: the entire (new) dead load had yet to be applied, and the new dead load that was in place was not in place symmetrically, laterally or longitudinally. Efforts to quantify the dead loads and construction live loads from photographs were inconclusive. Eventually, the quest to model and identify the lack of uplift was abandoned in favor of returning the bridge to its correct geometry as quickly as possible. Since the force needed to jack the bridge ends back to the correct elevations was not known, the contractor and steel erector suggested utilizing the 100-ton jacks that were already on site. Based on the effective cylinder area of the jacks and the observed pressure, only 29 kips of force were required to restore the bridge to its original position.



**Figure 11: One of the two jacks and cribbing used to restore the bridge to its correct geometry.**

Numerous attempts to reconcile the 29-kip load with the known bridge loads and geometry were unsuccessful. To date, the author has been unable to find why the bridge deflected the wrong way. This explanation is offered: at that point in time, the combination of partial dead loads and construction live loads on the bridge was simply not enough to result in the dead load uplift at the end of the bridge. This may be because of that particular arrangement of the loads being heavier in the flanking spans than in the main span during construction. In this case, the end span of the bridge seemed to behave like a cantilevered beam restrained at its end by an inclined reaction (this reaction being the suspension chain).

Another possibility may be due to load imbalance that was caused by the temporary scaffolding under the bridge during construction. A corrugated steel decking system (underdecking) running the full width and length of the bridge was in place when the old tie-downs were severed. Since the construction live loads acting on the underdecking are in a constant state of flux (including paint blasting media, damaged material removed from the bridge and replacement material staged for replacement, construction workers, among other loads) it is very likely that, again, the particular state of the temporary scaffolding system could have caused a load that was sufficient to overcome the permanent dead load uplift of the bridge in its final condition.

Whatever the cause, the designers agreed that the best course of action was to correct the geometry of the bridge immediately, and as the remainder of the loads were applied the uplift reaction would manifest as it was predicted.

## Summary

An overview of the analysis and rehabilitation of a self-anchored suspension bridge is presented. Because this is a unique structural system, extensive research was undertaken to understand the behavior of self-anchored suspension bridges and to better predict the response of the structure to applied loads.

The analysis of the bridge, using both finite element modeling and hand calculation, gave incredible insight into the behavior of this somewhat rare bridge type. The hand calculation especially required extensive derivation of the equations for the forces within the structure, an exercise that was commonplace in the past but which many younger engineers take for granted, with the prevalence of extremely powerful computers and analysis software.

Even with careful design and planning, several issues were encountered during construction that required careful consideration when planning their repair/resolution. A key takeaway of this project, for any bridge that uses a tie-down mechanism anywhere along its length that may warrant repair or replacement (self-anchored bridges, extradosed or cable-stayed bridges, some trusses) requires extremely careful consideration of the construction loading and timing of the repair. An exceptional degree of coordination and cooperation with the contractor should be exercised to ensure that the limitations of the repair work and loading are clear.

## Acknowledgements

The author would like to extend his humble thanks to the staff of the Allegheny County Department of Public Works (the Bridge Owner), the staff of the Pennsylvania Department of Transportation Engineering District 11-0 (the Program and Contract Manager), and the employees of Midas Information Technology, developers of Midas/Civil finite element analysis software, who worked in close collaboration with Michael Baker staff to correctly model and analyze the bridge behavior.

In addition, the author would like to thank his colleagues at Michael Baker International for their assistance and support during the design and construction phases of the project.

## References

- (1) Hawley, H. (1998). "Three Sisters Bridges." Historic American Engineering Record, National Park Service, Washington, D.C.
- (2) Lindenthal bridge photo, Carnegie Museum of Art Collection of Photographs, 1894 – 1958, Carnegie Museum of Art. <https://historicpittsburgh.org/islandora/object/pi%3A85.4.8>.
- (3) Hawley, H. (1998). "Three Sisters Bridges." Historic American Engineering Record, National Park Service, Washington, D.C.
- (4) Ibid.
- (5) Ibid.
- (6) Covell, V. R. (1926). "Erecting a Self-Anchored Suspension Bridge – Seventh Street Bridge at Pittsburgh." Engineering News Record 97:502.
- (7) Ibid.
- (8) Gronquist, C. H. (1942). "Simplified Theory of the Self-Anchored Suspension Bridge." Transactions. ASCE.
- (9) Wollman, Gregor. (2001). "Preliminary Analysis of Suspension Bridges." Journal of Bridge Engineering. ASCE.
- (10) Wollman, Gregor. (2001). "Self-Anchored Suspension Bridges – Discussion by Gregor P. Wollman, Member, ASCE." Journal of Bridge Engineering. ASCE.
- (11) Allegheny County Department of Public Works, Pittsburgh, PA. Original bridge calculation package.
- (12) Steinman, David B. (1922). A Practical Treatise on Suspension Bridges: Their Design, Construction, and Erection. John Wiley and Sons, New York.